RevMexAA (Serie de Conferencias), **41**, 28–31 (2011)

HOW TO USE ACTIVE OPTICS SHACK-HARTMANN DATA TO MEASURE THE SEEING AT THE FOCAL PLANE OF A TELESCOPE

P. Martinez,[1] J. Kolb,[2] M. Sarazin,[2] and J. Navarrete[3]

RESUMEN

Actualmente las estimaciones de seeing en tiempo real en el foco de un telescopio se enfatizan fuertemente ya que este conocimiento determina el dimensionamiento de los sistemas de óptica adaptativa (OA) y los aspectos operacionales de los instrumentos. En este contexto se estudia el interés de usar imágenes de OA del sensor Shack-Hartmann (SH) para proporcionar una estimación exacta del seeing. El sensor SH prácticamente entrega PSFs correspondientes a exposiciónes largas –en el lugar crítico del foco del telescopio– las cuales estan directamente relacionados con el seeing atmosférico en la línea de visión. Aunque los sensores SH no están especificados para medir los tamaños de PSFs sino las pendientes, se muestra que pueden obtenerse estimaciones exactas de seeing a partir de imágenes SH con un algoritmo especializado. Se analiza la sensibilidad de este algoritmo a varios parámetros de forma sistemática, demostrando que se puede obtener una estimación eficiente del seeing con una calibración adecuada.

ABSTRACT

Real-time seeing estimation at the focus of a telescope is nowadays strongly emphasized as this knowledge virtually drives the dimensioning of adaptive optics systems and instrument operational aspects. In this context we study the interest of using active optics Shack-Hartmann (SH) sensor images to provide accurate estimate of the seeing. The SH practically delivers long exposure spot PSFs –at the critical location of the telescope focus– being directly related to the atmospheric seeing in the line of sight. Although SH sensors are not specified to measure spot sizes but slopes, we show that accurate seeing estimation from SH images can be obtained with a dedicated algorithm. The sensitivity of this algorithm to various parameters is analyzed in a systematic way, demonstrating that efficient estimation of the seeing can be obtained with adequate calibration.

Key Words: instrumentation: adaptive optics — site testing

1. INTRODUCTION

The evaluation of the seeing is paramount for selecting astronomical sites and following their temporal evolution. Its estimation is also fundamental for the dimensioning of adaptive optics systems and their performance predications. This knowledge virtually drives instruments operational aspects at a telescope, and more emphasis is made to develop and use accurate real-time seeing estimator at the focus of the telescope.

The atmospheric seeing can be deduced from the width of the long-exposure PSF assuming successive corrections to apply (outer scale, wavelength, and airmass). For this purpose, several flavors of images can be used at the critical location of the telescope focii: (1) scientific instruments images, (2) guide probe images, (3) active optics Shack-Hartmann images. However seeing estimation from the width of PSF strongly rely on the exposure time that must be long enough so that the turbulence have been averaged (i.e., all representations of the wavefront spatial scales have passed through the pupil). This already discard the use of the guide probe as exposure time are not longer than 50 milli-second, while scientific instrument images do not entirely comply with the real-time aspect of the seeing estimation as they are affected by an observational bias (i.e., unavailability for a large range of seeing conditions) and are affected by the telescope field stabilization.

At the VLT, the Active Optics Shack-Hartmann (SH) sensor measures aberrations and corrects them by deforming the active primary mirror of the telescope. Slopes are used for this measurement, while the average spot size in the sub-apertures is measured and stored as diagnostic since the commissioning of the VLT. Because the SH delivers continuously real-time images of long exposure spot PSFs (typically 45 seconds) and spot sizes are directly related

[1]UJF-Grenoble 1, CNRS-INSU, Institut de Planétologie et d'Astrophysique de Grenoble (IPAG) UMR 5274, Grenoble, F-38041, France.

[2]European Southern Observatory, Karl-Schwarzschild-Strasse 2, D-85748, Garching, Germany.

[3]European Southern Observatory, Alonso de Cordova 3107, Casilla 19001, Vitacura, Santiago, Chile.

to the atmospheric seeing in the line of sight, such images provide an advantageous access to the seeing at the focal plane of the telescope, where scientific instruments are located. In this study we present and discuss calibrations and tests of an algorithm developed to accurately determine the width of long exposure SH spot PSFs with the goal of providing an estimate of the seeing at the telescope focii.

2. EXTRACTING SEEING FROM SPOT SIZES

2.1. *Prerequisite: seeing and image quality*

The full width at half maximum (FWHM) of a long-exposure stellar image –also called image quality– is commonly considered to be equal to the atmospheric seeing. However the outer scale of the turbulence (L_0), which corresponds to a reduction in the low frequency content of the phase perturbation spectrum, plays a significant role in the improvement of image quality at the focus of a telescope. The image quality is therefore different (and in some cases by a large factor) from the atmospheric seeing that can be measured by dedicated seeing monitors, such as a differential image motion monitor (DIMM, Sarazin & Roddier 1990). The dependence of atmospheric long exposure resolution on L_0 is efficiently predicated by a simple approximate formula (equation 1) introduced by Tokovinin (2002), and recently verified by means of simulations (Martinez et al. 2010a,b) where we emphasized that the effect of finite L_0 is independent of the telescope diameter

$$\mathrm{FWHM} \approx \varepsilon_0 \sqrt{1 - 2.183(r_0/L_0)^{0.356}}\,. \tag{1}$$

As a consequence, to deduce atmospheric seeing ε_0 (at 0.5 μm) from the FWHM of a long-exposure PSF the correction implied by equation 1 is mandatory prior to airmass and wavelength correction.

2.2. *Algorithm principle*

At the VLT, long exposure SH images are recorded with typical exposure time of 45 seconds, long enough so that the turbulence has been averaged. The algorithm has been proposed by Tokovinin et al. (2007) and is described in the following. Background estimation is performed on a corner of the image without spots, and hot pixels are set to the background. Only the sharpest, unvignetted spots are selected in each frame for the analysis. These extracted spots are oversampled by a factor 2, re-centered and averaged. The averaging reduces the influence of potential local CCD defects (e.g, bad pixels, bias structures, etc.). The modulus of the long-exposure optical transfer function (OTF) of the averaged spot is calculated and normalized. It is then divided by the square sub-aperture diffraction-limited transfer function, and fitted by a 2D Gaussian function from which the SH spot profile is determined. FWHM of the small and large axis are then extracted.

3. SIMULATION HYPOTHESIS

In the following we consider a telescope pupil diameter of 8 m (VLT Nasmyth focus), and a wavelength of 0.5 μm.

3.1. *Shack-Hartmann model*

Our simulations are based on a diffractive Shack-Hartmann (SH) model that reproduces the VLT active optics SH geometry: 24 sub-apertures over the pupil diameter, 22 pixels per sub-aperture, 0.305$''$ pixel scale, $d = D/24 = 0.33$ m. The validity of the SH model has been verified on several aspects such as the plate scale, spot sizes, slope measurements, and phase reconstruction.

3.2. *Atmospheric turbulence*

The atmospheric turbulence is simulated by 300 uncorrelated phase screens of dimension 3072×3072 pixels (i.e. 45 meters width). The principle of the generation of a phase screen is based on the Fourier approach: randomized white noise maps are colored in the Fourier space by the turbulence power spectral density (PSD) function, and the inverse Fourier transform of an outcome correspond to a phase screen realization. Verification have been carried out on the phase screens to ascertain the value of the input outer scale (L_0), Fried parameter (r_0) and seeing, such as decomposition on the Zernike polynomials and variance measurements over the 300 uncorrelated phase screens. In addition the validity of the long-exposure SH image has been verified.

4. RESULTS

The sensitivity of several parameters has been analyzed to properly characterize the FWHM estimation algorithm. This calibration process is a prerequisite step prior to on-sky implementation of the algorithm. For this calibration process we considered the impact of several important parameters such as: the turbulence outer scale, the telescope field stabilization, the sampling of the SH spots, the elongation of the spots (i.e., the atmospheric dispersion), the PSF contribution of the detector, and the detector read-out noise.

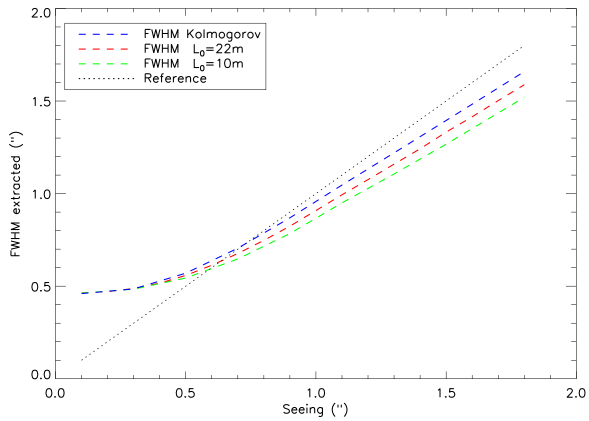

Fig. 1. Impact of the turbulence outer scale on the seeing estimation.

4.1. *Outer scale*

In Figure 1 the extracted FWHM as function of the phase screen seeing is shown for several L_0 values (10 m, 22 m, and Kolmogorov case, i.e., infinite outer scale although likely about 200 m due to the physical size of the phase screens). The algorithm provides a smooth response to seeing although two regimes are observable: (1) when the seeing is better than $0.6''$ the FWHM is overestimated due to the under-sampling (pixel scale is $0.305''$), (2) when the seeing degrades further than $0.6''$ the FWHM is underestimated and asymptotically converges towards equation 1. In addition, it is established that SH sub-apertures are not small enough so that FWHM $\approx \varepsilon_0$, i.e., the SH spot FWHM measurements depend on the outer scale.

4.2. *Spot sampling*

To understand the asymptotical trend of the algorithm response to seeing presented in the previous subsection, we analyze the effect of the spot sampling on the FWHM measurement. Results are presented in Figure 2 (top) where it is shown that for a given seeing, the estimation gets better with the sampling. FWHM at $0''$/pixel sampling corresponds to theoretical values obtained with equation 1. A rough estimation indicates that 5 pixels per FWHM is required for accurate measurement, although it can be calibrated and corrected in case of poor sampling.

4.3. *Field stabilization*

The telescope field stabilization removes the low frequency Tip-Tilt components generated by, among other things, wind shacking and telescope vibrations. As a consequence the field stabilization also removes the slow turbulence, which potentially may reduce the FWHM of a PSF image, and therefore the FWHM of the SH spots.

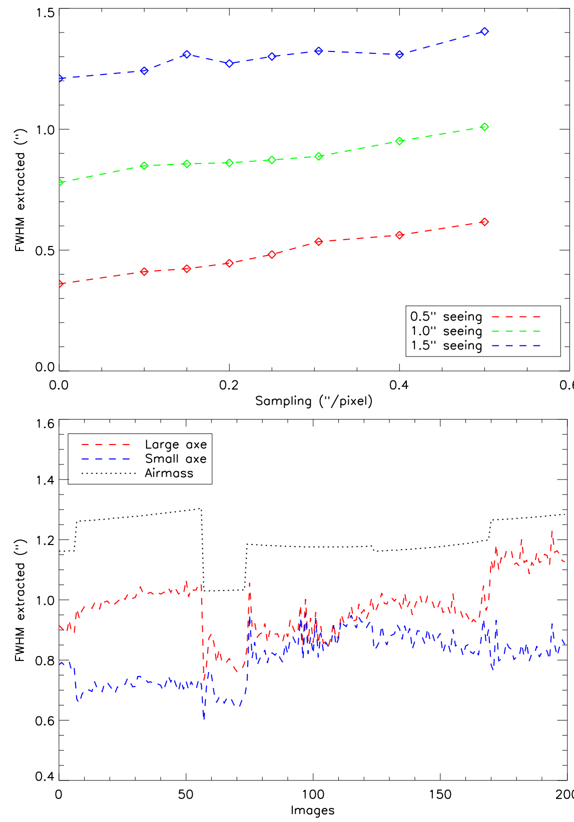

Fig. 2. Top: Impact of the SH spot sampling on the seeing estimation (simulated data). Bottom: Impact of the uncorrected atmospheric dispersion on the seeing estimation (real data).

To assess the impact of the field stabilization we compare the FWHM measurements on simulated SH images where the Tip-Tilt (in the full telescope pupil) has been completely removed (worst case: perfect field stabilization with infinite bandwidth) to that of SH images not modified. This test has been carried out for several seeing conditions (0.1, 0.9, $1.8''$) and outer scale values (10 m, 22 m, and Kolmogorov case). No impact has been revealed. The estimation of the seeing from the width of SH spots is therefore not affected by the field stabilization, which rises as a relevant advantage.

4.4. *Atmospheric dispersion*

Except for data taken at zenith, individual spot in SH images can exhibit elongation in one direction due to uncorrected atmospheric dispersion. The algorithm allows the estimation of FWHM in two orientations, small and large axes. The algorithm has been applied on 200 real SH images obtained at the VLT-UT3 Nasmyth focus (not equipped with an atmospheric dispersion compensator) on May 12th 2010. Results of the FWHM extracted along the small and large axis are presented in Figure 2 (bottom) where the airmass is over-plotted. The algorithm does differentiate the elongated axis, and for both axis it follows the evolution of the airmass. The difference between the two axis can be as large as 0.3″ which is definitely not negligible.

4.5. *Detector PSF*

The diffusion of charges in the detector material before they are allocated to one pixel is observable as an artificial enlargement of the PSF. In most cases, the spatial response of the detector is not trivial to determine and is indeed unknown for the detector of the active optics SH at the VLT. Figure 3 (top) presents the impact of the detector PSF on the measured FWHM in the case of 1″ seeing. We found that the detector PSF enlarges the FWHM and that the effect can be significant. It starts to be not negligible from 1 pixel although it is reasonable to consider that its impact regardless the amplitude can be calibrated.

4.6. *Signal-to-noise*

At the VLT the read-out-noise (RON) level of the active optics SH is above 15 ADUs, while typical signal is about 20000 ADUs per sub-apertures. In Figure 3 (bottom) we present the measured FWHM in the case of 1″ seeing as a function of the signal level (in ADUs) for a RON of 15 ADUs. It is shown that poor signal-to-noise ratio image enlarges the FWHM which is evident for signal lower than 10000 ADUs, while for signal higher than 10000 ADUs the FWHM measurements is roughly stable. The standard signal ADU level obtained at the VLT is therefore high enough to avoid any impact on the FWHM estimation, although it can be calibrated otherwise.

5. CONCLUSION

Active Optics SH images offer an advantageous possibility to estimate the seeing at the focus of a telescope. We show that although the algorithm is sensitive to several parameters it can be calibrated to accurately retrieve the seeing from the SH images.

We found that active optics SH is not sensitive to the telescope field stabilization, and that even considering the small size of the SH sub-apertures, it does depend on the turbulence outer scale L_0 and therefore follows equation 1.

Therefore Active Optics SH can be used to build statistics using median value of L_0, and in a real-time fashion but relying on median L_0 value, or requiring

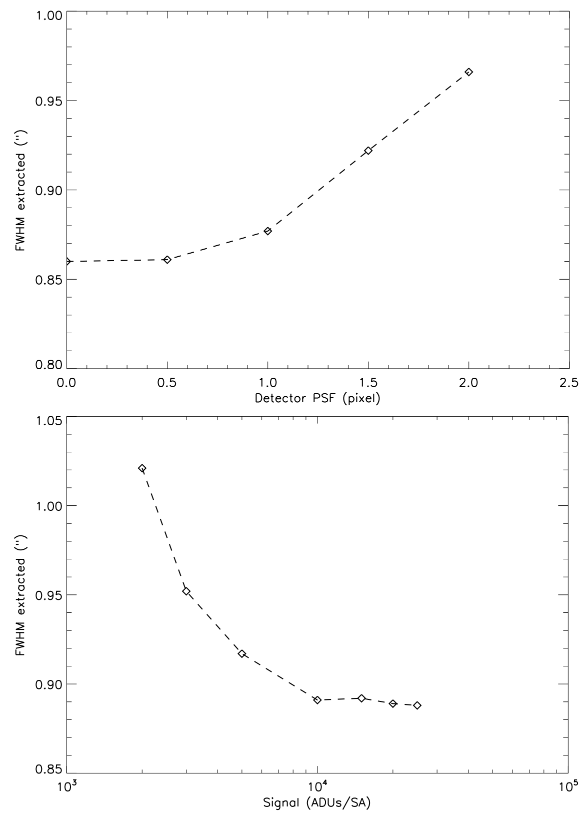

Fig. 3. Top: Impact of the detector PSF on the seeing estimation. Bottom: Impact of the signal-to-noise (RON=15ADUs) on the seeing estimation.

instantaneous measurement of L_0. We note that in this context several independent campaigns have converged to the median value of L_0 of 22 m at Paranal (e.g., Dali Ali et al. 2010).

The qualification and calibration aspects of the algorithm presented in this study is nearly completed and clear the path to its operational implementation at the VLT for a year of test period starting in fall 2011. Finally, we note that more emphasis is given to use closed-loop real-time AO instruments data in the near future to get the estimate of the seeing at the critical location of the telescope focus.

REFERENCES

Dali Ali, W., et al. 2010, A&A, 524, A73
Martinez, P., Kolb, J., Sarazin, M., & Tokovinin, A., 2010a, The Messenger, 141, 5
Martinez, P., Kolb, J., Tokovinin, A., & Sarazin, M., 2010b, A&A, 516, A90
Sarazin, M., & Roddier, F. 1990, A&A, 227, 294
Tokovinin, A. 2002, PASP, 114, 1156
Tokovinin, A., Sarazin, M., & Smette, A. 2007, MNRAS, 378, 701